• Article •

Cluster of solar active regions and onset of coronal mass ejections

WANG JingXiu[1*], ZHANG YuZong[1], HE Han[1], CHEN AnQin[2], JIN ChunLan[1]
& ZHOU GuiPing[1]

[1] *Key Lab of Solar Activity, National Astronomical Observatories, Chinese Academy of Sciences, Beijing 100012, China;*
[2] *National Center for Space Weather, China Meteorological Administration, Beijing 100081, China*

Abstract round-the-clock solar observations with full-disk coverage of vector magnetograms and multi-wavelength images demonstrate that solar active regions (ARs) are ultimately connected with magnetic field. Often two or more ARs are clustered, creating a favorable magnetic environment for the onset of coronal mass ejections (CMEs). In this work, we describe a new type of magnetic complex: cluster of solar ARs. An AR cluster is referred to as the close connection of two or more ARs which are located in nearly the same latitude and a narrow span of longitude. We illustrate three examples of AR clusters, each of which has two ARs connected and formed a common dome of magnetic flux system. They are clusters of NOAA (i.e., National Oceanic and Atmospheric Administration) ARs 11226 & 11227, 11429 & 11430, and 11525 & 11524. In these AR clusters, CME initiations were often tied to the instability of the magnetic structures connecting two partner ARs, in the form of inter-connecting loops and/or channeling filaments between the two ARs. We show the evidence that, at least, some of the flare/CMEs in an AR cluster are not a phenomenon of a single AR, but the result of magnetic interaction in the whole AR cluster. The observations shed new light on understanding the mechanism(s) of solar activity. Instead of the simple bipolar topology as suggested by the so-called standard flare model, a multi-bipolar magnetic topology is more common to host the violent solar activity in solar atmosphere.

activity, coronal mass ejection, magnetic fields

PACS number(s): 96.12.Hg, 96.12.Jt, 96.12.Kz

1 Introduction

No longer limited by observations of an isolated active region (AR), a new vision on solar activity comes up to solar astronomers by space-borne observations with full-disk coverage of the solar magnetic field and multi-wavelength images. The solar activity events often involve more global magnetic connectivities and interactions of a few ARs as well as quiet regions simultaneously. Large-scale coronal connectivity was revealed in coronal mass ejections (CMEs)

(Wang et al. [1,2]; Zhang et al. [3]; Zhou et al. [4]; Schrijver and Title [5]; Schrijver et al. [6]). Observations of extreme-ultraviolet (EUV) irradiance from Solar Dynamic Observatory (SDO, Pesnell et al. [7]) have disclosed the flare late-phase events indicating the interactions of multi-scale and different-height magnetic loop systems (Woods et al. [8]; Woods [9]). Even before the launch of SDO, in a case study Wang et al. [2] clearly demonstrated that flares in an AR, i.e. NOAA AR10696, were followed by either a trans-equatorial flare/CME or an eruption of a trans-equatorial filament/CME with a large scale and a long duration of more than 10 h. The trans-equatorial activity showed exactly a flare late-phase enhancement in the EUV light

---

*Corresponding author (email: wangjx@nao.cas.cn)

curve, as that reported by SDO/EVE observations. The trans-equatorial structures and activities are closely associated with the magnetic field of AR 10696 where the flare began first. These new observations, in particular, the SDO/AIA (i.e., Atmospheric Imaging Assembly; Lemen et al. [10]) observations have revealed the overall magnetic connectivity among ARs, as well as, coronal holes and quiet regions (Wang and Jiang [11]).

However, to theoretically describe and model the complex topology rather than a simple magnetic dipole is not an easy task. For the simplest case of multi-bipolar field interaction, the magnetohydrodynamic (MHD) catastrophe in a quadrupole configuration in which there is an emerging flux rope had been modeled numerically (Zhang et al. [12,13]; Zhang and Wang [14]). These authors found a doubled-catastrophe of the flux rope which resulted in the formation of two current sheets, one of which was horizontal current sheet covering the overall two bipolar flux systems and the other was underneath the flux rope like that in the standard flare model. Based on the MHD numerical simulation, these authors proposed a two-current-sheet CME model which could reproduce both the magnetic breakout scenario of CME and the scenario predicted by standard flare model. Longcope and Forbes [15] later developed general analytical models of two-current-sheet flare/CME for the same quadrupole magnetic configuration. Kliem et al. [16] considered both the simple bipolar and the quadrupolar cases and discussed in detail the MHD instability, e.g., the catastrophe, kink and torus instability, which would be responsible for the onset of CMEs.

In this paper, we describe a new type of magnetic complex: the cluster of ARs (abbreviated as AR cluster). An AR cluster consists of two (or more) ARs which are located in the same activity belt and magnetically connected, forming a relatively separate dome of magnetic flux system. In the multi-wavelength EUV observations, the clustered ARs show overall-connected bright structures which are separated from the dimmer surroundings. The CME onset in an AR cluster often takes place in the interacting magnetic field of the two partner ARs.

In AR clusters, there are two types of interacting magnetic field, which are of fundamental importance for CME initiation. One type is the AR-inter-connecting loops which link the opposite magnetic fields of the two clustered ARs. In short, we call them inter-connecting loops. Another type is the channeling filament which lies above the neutral channel of opposite magnetic fields of the two clustered ARs. We call them channeling filament. We will demonstrate that the breakout of inter-connecting loops and the eruption of channeling filaments would define the onset of CMEs in AR clusters.

The next section is devoted to the description of AR cluster. We show three examples of AR clusters which are composed of ARs 11226 & 11227, ARs 11429 & 11430, and ARs 11515 & 11514, respectively. In sect. 3, we pre-

sent evidence that the CME onset is closely associated with either the breakout of inter-connecting loops or the eruption of channeling filaments. In the last section, we draw the conclusion and present a brief discussion.

2   AR clusters

An AR cluster consists of two or more interacting ARs. The partnering ARs have almost the same latitude and a small span of longitude. In the full-disk EUV images of high spatial resolution and sensitivity, as obtained by SDO/AIA, an AR cluster manifests as a domain of interconnected bright structures, which is separated from the relatively dim surroundings.

Three selected examples of AR clusters are shown in Figure 1 with SDO/HMI (i.e., Helioseismic Magnetic Imager) magnetograms and SDO/AIA 131 Å images. The selected AR clusters are relatively simple ones, and each of them only consists of two ARs, i.e., ARs 11226 & 227, ARs 11429 & 430, and ARs 11515 & 514, respectively. In each cluster, the component ARs are closely packed in both latitude and longitude. According to the NOAA AR list, for the AR clusters 11226 & 227, 11429 & 430, and 11515 & 514, the latitude differences of two partner ARs are $\delta\Phi \approx 3°$, 3°, and 1°, respectively; and the longitude differences are $\delta\vartheta \approx$ 12°, 15°, and 12°, respectively. It is speculated that the clustered ARs stem from the same bundles of magnetic lines of force below the photosphere, as they almost have the same heliographic latitudes and very narrow range of longitudes.

Unfortunately, we can only view the magnetic connectivity from the full-disk multi-wavelength images as that shown in the 131 Å images (Right panel of Figure 1), which represent the plasma structure in the temperature range with peak temperature distribution at about 2×10^7 K. For understanding the magnetic connectivity, we have to consider and adopt a fact that above the solar chromosphere the plasma is frozen into the magnetic lines of force, as the plasma $\beta \ll 1$ there. Therefore, basically the EUV structures are tracing the magnetic lines of force. From the 131 Å images, we were able to see the overall connections of the hot, condensed and bright loops between the two clustered ARs.

A reliable way to view the magnetic connectivity in the solar atmosphere is based on the three-dimension (3D) theoretical extrapolation of the photospheric vector magnetograms into the corona. A commonly accepted numerical approach is the extrapolation based on the assumption of non-linear force-free (NLFF) magnetic field in the solar chromosphere and corona.

Here, we show a NLFF extrapolation for AR cluster 11515 & 514 (Figure 2) by using the surface element method (Yan and Sakurai [17]; He et al. [18]). The extrapolation clearly reveals the magnetic connectivity of the two
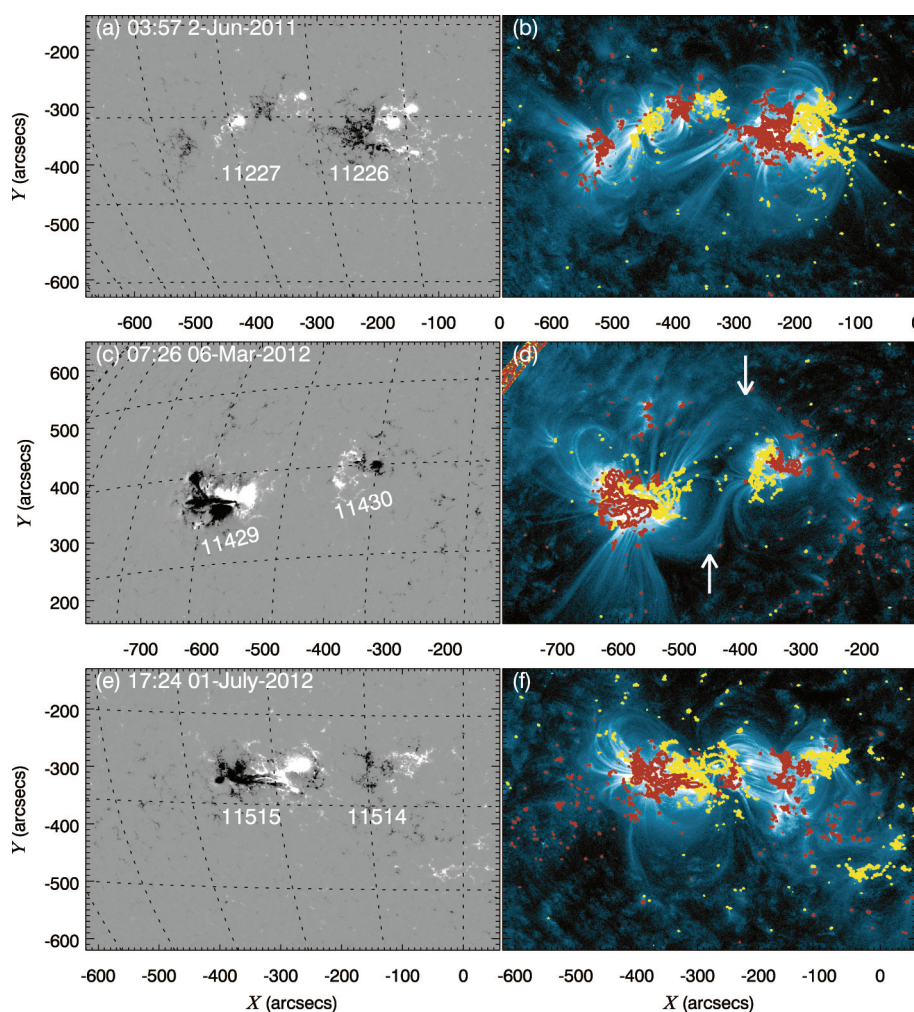
Figure 1   (Color online) Three AR clusters whose component ARs are listed by NOAA AR numbers. Left panel: HMI line-of-sight magnetograms displayed in the range of ±500 G, on which grids with 10° separation in latitude and longitude are shown by thin white dotted lines. Right panel: AIA 131 Å images on which iso-Gauss counters of ±200, 1000 G are superposed by yellow and red lines. Two arrows in the figure indicate the inter-connecting loops linking the opposite polarity fields, respectively, from ARs 11429 and 11430. In this and following figures, the locations of the ARs are denoted in the *X* (east to west) and *Y* (north to south) coordinates by the arcsecs from the disk center.

clustered ARs. The connectivity manifests in two forms: (1) arcades connecting the opposite polarity fields of the two ARs and (2) a magnetic flux rope in the neutral channel of the two ARs. In Figure 2, we saw the abundance of magnetic lines of force which were connecting the positive magnetic flux of the main sunspot of AR 11515 and the negative magnetic flux of AR 11514 (see the long arrow in the upper panel). They are the inter-connecting loops. More interestingly, a magnetic flux rope underneath the arcades has been disclosed by the extrapolation (see the lower arrow in the upper panel). The flux rope appears as a sigmoidal structure and has been found to erupt many times in the later evolution of the cluster. In this AR cluster, the inter-connecting magnetic loops and their underlying flux rope play a very active role in driving flare/CME events (see an example described in the next section).

The magnetic flux rope or rope-like structure in an AR cluster is commonly seen between the two component ARs.

In AR cluster AR 11226 & 227, a filament has been identified (see Zhang et al. 2014, submitted to Astron Astrophys), whose western piece was formed by the interaction between the negative magnetic flux of AR 11226 and the positive magnetic flux of AR 11227 (Figure 3). Together with the eastern piece of the filament which was formed between opposite polarity fields within AR 11227, the filament appeared in a fully circular shape. Moreover, the two pieces of the filament responded to the photospheric magnetic field evolution separately and erupted successively, which caused two small flares and CMEs. The eastern piece of the filament erupted first, associated with a C1.4 flare and a partial halo CME; the western piece erupted later and more violent, while associated with a C3.7 flare and a halo CME. The lower panel of Figure 3 shows the earliest eruption of the western piece filament. It appears like an S-shaped twisted rope with intertwined brightened and darkened threads, while the arcades are still seen to overlie above the filament.
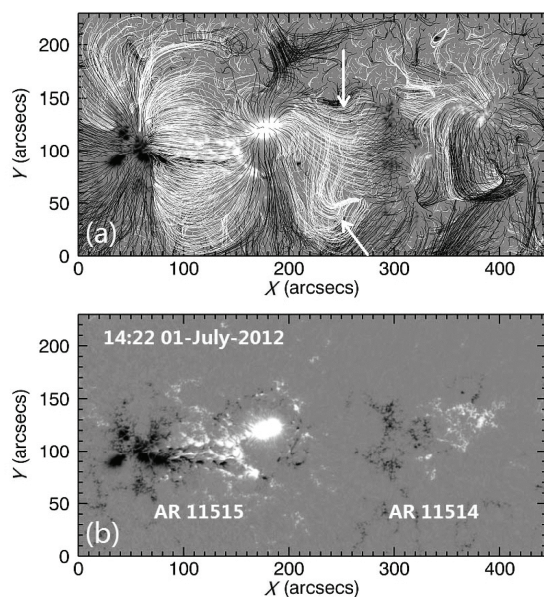
Figure 2 Extrapolated magnetic lines of force (viewed from above) of AR clusters 11515 & 514 (Top panel) from the HMI vector magnetograms taken at 14:22 UT on July 1, 2012. The vector magnetogram data have been corrected for projection effect. The relevant line-of-sight magnetograms are shown in the range of ±1500 G (lower panel) with brighter (darker) patches for positive (negative) magnetic flux.
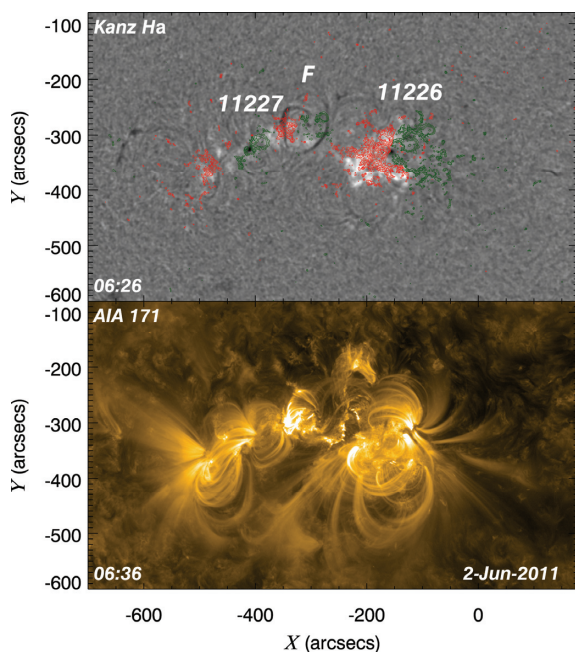

Figure 3 (Color online) Upper panel: Hα image showing the filament marked by "F" as circular darker features. Magnetic flux distribution is shown by iso-Gauss contours of ±100, 500, 1000, 1500 G with green (red) lines for positive (negative) polarity. Lower panel: AIA 171 Å image showing the eruption of the filament at the earliest stage.

It is very interesting to notice that the flare has ribbons in both ARs. Therefore, even for such a small flare, it is not physically constrained in a single AR. This fact is very inspiring and elucidating in understanding flare magnetism or

mechanisms. The involvement of different flux systems is a key fact in flare scenario.

There are, at least, two different types of magnetic configurations and topology skeletons in AR clusters. The clusters 11515 & 514 and 11226 & 227 show a parallel magnetic orientation of the two component ARs. Each magnetic bipole in the cluster follows the regularity that the preceding polarity was followed by the following polarity in the given solar hemisphere. The configuration for this quadrupole field is very close to the descriptions of Zhang et al. [12], Kliem et al. [16], and Longcope and Forbes [15] (see the discussion by Wang and Jiang [11]). However, in AR cluster 11429 & 430, one partner AR 11429 has an inverted magnetic orientation. As the clustered ARs are located in the northern hemisphere, the preceding magnetic polarity is negative. However, in AR 11429 this regularity was broken. Its following (positive) polarity was in front of the preceding (negative) polarity. The magnetic connectivity is different from that described for AR cluster 11515 & 514 previously (see Figure 2). One fact is unavoidable that in the AR cluster 11429 & 430 there must have been two bundles of magnetic lines of force, encountering in the corona with opposite field direction (see the two inter-connecting loops indicated by the arrows in the right panel of Figure 1). The reconnection between the two bundles of opposite directed lines of force will favor the breakout of the overall magnetic structures for the onset of CMEs. An analysis of the magnetic connectivity and magnetism of flare/CME in this magnetic configuration will be detailed in the next approach.

3   CME Initiation in AR clusters

Case and statistical studies of flare/ CME initiation in complicated magnetic configurations have been presented in many studies (Zhang et al. [19]; Wang et al. [20,21]; Wen et al. [22]; Zhou et al. [4]; Zhang et al. [3]; Zhang et al. [23]; Chen et al. [24]; Chen and Wang [25]; Nitta et al. [26]; Vemareddy et al. [27]; Grechnev et al. [28]), see also a review by Wang and Ji [29]. However, in the previous studies, the evidence on how the magnetic connectivity between two or more ARs is closely related to flare/CME onset is very rare. Often a study is too much concentrated on the fine details of the magnetic and brightness structures without a vision on the fundamental magnetic topology.

Here, we report a definitive example that the eruption of the AR-inter-connecting loops between two clustered ARs is associated with the initiation of a CME (see the time-sequence in Figure 4). The overall scenario of the inter-connecting loop eruption consists of several steps: growth, early eruption, disappearance and post- eruption.

The inter-connecting loops grew for more than 8 h, approximately from 06:10 UT to 14:52 UT. The growth of the inter-connecting loops was temporally correlated with an

emergence of the flux rope underneath the loop sets (see an arrow at 12:28 UT and refer Figure 2). During this interval, many jets were seen from the footprints of the emerging flux rope. The earliest eruption of the inter-connecting loops is shown as an ejection from its left footpoints in AR 11515 at 14:55 UT (see the arrow at 14:55 UT), and then the loops suffer from a temporary collapse before an ejection from the right foot-points in AR 11514 at 15:16 UT. A complete eruption of inter-connecting loops followed afterwards. A 'post-flare' like brightening manifested as sheared and twisted structures was seen in association with the emerging flux rope since 15:43 UT, following the eruption. The post-eruption structures become more potential later. From 16:10 UT to 16:43 UT, post-eruption brightening loops appeared progressively in the AR 11515 and AR 11514, respectively.

The main three magnetic connections, i.e., the inter-connecting loops between two ARs, AR 11515 and AR 11514, all became brightened successively (see the three yellow arrows at 16:16 UT), resembling the usual post-flare loops in an AR. From the earliest eruption of inter-connecting loops to the latest post-eruption brightening in AR 11514, however, only a C8.2 flare (15:41 UT to 15:52 UT)
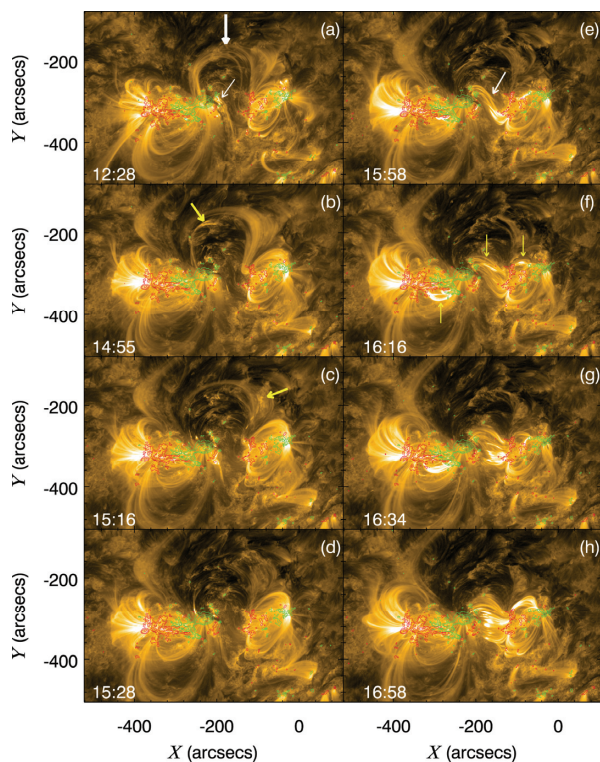
in AR 11515 and a partial halo CME (in C2 field of view at 15:36 UT observed by Large Angle and Spectrometric Coronagraph Experiment) with a linear speed of 723 km s^{-1} were recorded in the NOAA database. A C2.4 flare (15:26 UT-15:37 UT) is diagnosed to be in AR 11513 but not in AR 11514 of the AR cluster. The whole duration of the activities in the AR cluster was approximately 2 h. To summarize, we list the key events in Table 1.

The backward extrapolation of the CME from the LASCO/C2 field of view locked its on-disk initiation in the tempo-spatial window of the eruption of the inter-connecting loops. This example elucidates how the magnetic fields in the AR cluster are inter-connected and coupled to initiate the panorama of activity. By the round-the-clock and full-disk observations of multi-wavelength images and magnetograms, we seem to be able, for the first time, to gain a vision on the real breeding ground of magnetic activity, which has multi-pole magnetic topology even though the activity events were not big. In the standard flare model only a bipolar field with a flux rope embedded is considered. The overall magnetic interaction in the multi-pole field has been largely ignored, so that it is difficult to interpret the simultaneous flare/CME occurrence and the sympathetic activities. However, the standard flare model does describe a central part of the overall scenario: the magnetic reconnection driven by an erupting flux rope is the key for the explosive magnetic energy release in solar activity.

Guided by the standard flare model, we can make a working hypothesis that the well-observed post-flare loops are the signature of magnetic reconnection at the current sheet above. Based on this hypothesis and considering the results of early 3D extrapolation (see Figure 2), we envision a multi-current sheet system (see a cartoon in Figure 5), which could interpret the observed activities in AR cluster AR11515 & 514. The emerging flux rope is visualized in the line-of-sight magnetogram as weak elongated flux of opposite polarity. In the pre-activity status, we have a horizontal layer of concentrated currents (see Figure 5). The emergence of the flux rope drives the magnetic breakout of the overall magnetic arcades (or the eruption of inter-connecting loops). This deforms the current concentrations into a current sheet system which is shown in the right panel

Figure 4   (Color online) Time-sequence of AIA 171 images showing an eruption of inter-connecting loops between ARs 11515 & 11514 (see the larger white arrow at 12:28 UT). Early ejections from footpoints of the inter-connecting loops are indicated by smaller yellow arrows at 14:55 UT and 15:16 UT, respectively. The instability of the emerging flux rope is shown by the two smaller white arrows at 12:28 and 15:58 UT. Three sets of post-eruption brightening loops are indicated by three yellow arrows at 16:16 UT.

Table 1   Scenario of the activity events in the AR cluster

| Time	Activity events
06:19–14:52	growing of Inter-connecting loops
14:52	ejection from the loop footpoint in AR 11515
15:16	ejection from the loop footpoint in AR 11514
14:52–15:25	complete eruption of inter-connecting loops
15:36 –	partial halo CME at C2 field of view
15:41–15:52	C8.2 flare in AR 11515
15:43 –	post-eruption brightening in inter-connecting loops
16:10 –	post-eruption brightening in AR 11515
16:43 –	post-eruption brightening in AR 11514
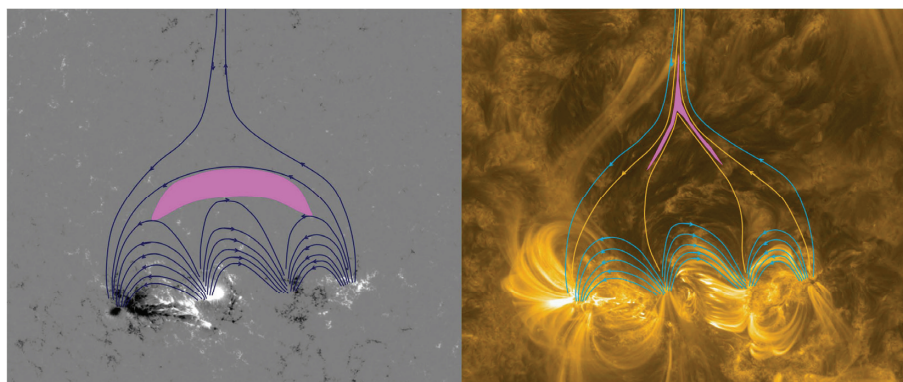
Figure 5   (Color online) Envisioned magnetic skeleton and current sheet (pink color) distribution before and after the eruption of the inter-connecting loops. The breakout of inter-connecting loops resulted in complicated current system and three sets of magnetic reconnection. The cartoon is drawn on the top of HMI magnetogram and AIA 171 Å image shown in previous figures.

of the figure. In fact, there are three current sheets which were formed during the eruption of overall arcades, and successive magnetic reconnections take place causing further acceleration of the CMEs and the flares in AR 11514 &11515, respectively.

In Figure 6, we show the eruption of inter-connecting loops in the AR cluster 11429 & 430. As we mentioned, the cluster consists of two ARs with opposite magnetic orientations. Therefore, there should be two sets of inter-connecting loops with opposite directions of magnetic field encountering in the corona (see the two arrows in the left panel of the figure, also see them in Figure 1). The dynamic formation and dissipation of current sheets are expected. The AR 11429 is the first super AR in solar cycle 24, produced three X-class X-ray flares and six high-speed CMEs with speed larger than 1000 km s^{-1}. The X1.3 flare on March 7, 2012 (started from 01:05 UT and peaked at 01:14 UT) is closely associated with the eruption of the in-

ter-connecting loops between the positive magnetic field of AR 11430 and the negative field of AR 11429. The eruption started at 01:03 UT before the X1.3 flare, and resulted in a large area of EUV dimming. Moreover, flaring is seen both in ARs 11429 & 430 during the inter-connecting loop eruption (see the right panel of Figure 6). To assign the flare solely to AR 11429 is not truly correct. An associated CME with a speed of 1825 km s^{-1} appeared first at C3/LASCO field of view at 01:30 UT. Again, we saw the evidence that the flare/CME is closely associated with the magnetic connectivity and interaction of the two clustered ARs.

As argued by Low [30], for the solar corona where the plasma tends to be fully ionized, its high conducting fluid could be sustained via the spontaneous formation and resistive dissipation of current sheets, and the coupling between the resistive induction and the dynamical formation and dissipation of current sheets becomes a key issue in solar activity study. To resolve the problem, the 3D radiative
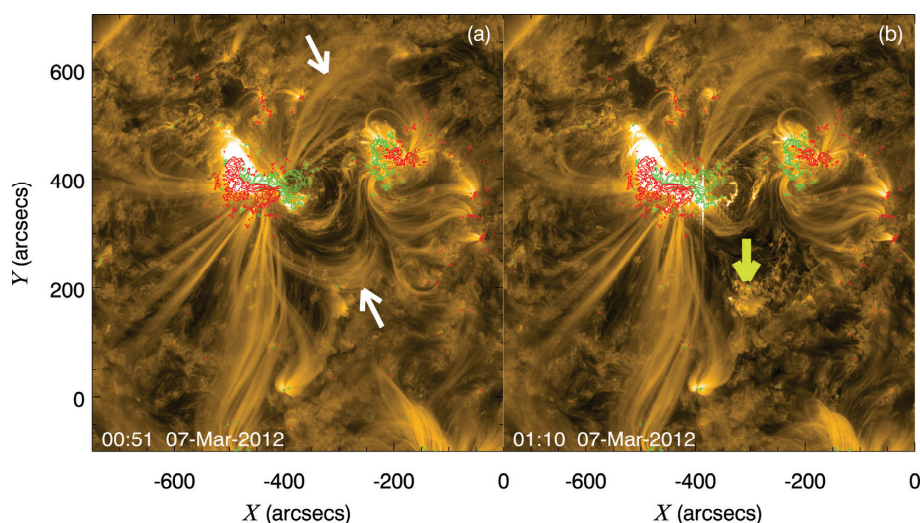

Figure 6   (Color online) Eruption of inter-connecting loops in AR cluster of 11429 and 430 and the X1.3 flare shown by AIA 171 Å image superposed by the magnetic flux density with green (red) lines for positive (negative) polarity and contours of ±200, 500, 1000, 1500 G. The two white arrows indicate the two sets of inter-connecting loops between two ARs and a heavy yellow arrow indicates the earliest eruption of one set of inter-connecting loops.

MHD simulation guided by careful observational diagnosis and thorough theoretical analysis would serve as a powerful tool.

4 Conclusion and discussion

In this paper, by virtue of SDO/HMI magnetogram and AIA images, we described a new type of magnetic complex: the cluster of solar ARs. A cluster of ARs consists of two or more ARs which are located in almost the same latitude and has a narrow range of longitude, e.g., within about the 30° of longitude. The clustered ARs form a common domain of magnetic flux system and show as bright structures roughly separated from its dimmer surroundings in EUV wavelengths. The interacting and coupling of the clustered ARs are realized by means of either the inter-connecting loops directly linking the opposite polarity flux of the two ARs, or the filaments or flux ropes channeling in the magnetic neutral zone of the two ARs.

We further exemplified that in all the three sampled AR clusters, at least, there were a few flare/CME events whose initiations were identified to definitively associate with either the breakout of AR-inter-connecting loops or the eruption of channeling filaments. For the illustrated examples, it is not correct to attribute or allocate the flare/CME to the magnetism of a single AR. By this study we learned that to thoroughly understand the mechanism or mechanisms of solar activity, we have to consider the truly complicated magnetic complex in which multi-bipolar flux systems are included and ultimately interacted. The recognition is of importance for considering the future development of prediction capability of solar activity and space weather. There are three points which should be discussed.

Firstly, the current study is not based on a large sample. Therefore it has no statistical basis to estimate how often we could have AR clusters and how many percentage of flare/CMEs are tied to AR clusters. On the other hand, more quantitative analyses are planned to get detailed knowledge on the triggering condition of the flare/CMEs in AR clusters.

Secondly, the AR clusters described in this paper occurred in 2011 and 2012 when the solar activity level was relatively low. There were not many ARs on the Sun on these occasions. Therefore, the AR clusters were isolated from their surroundings. They are easily identified by examining the magnetograms and EUV images. The magnetic connectivity between two clustered ARs is clear and neat for physical understanding. We would probably see many ARs on the Sun when the Sun's activity level rose to very high level, and the magnetic connectivity would be more complicated. CME initiation in such a complicated magnetic complex would be very interesting for further analysis.

Finally, we shall mention that the AR cluster described in this paper is a new revelation of magnetic complex in solar activity study. The analysis here is concentrated on the magnetic connectivity between ARs. This magnetic complex is, in particular, distinctive to a magnetic bipolar region. Multipole topology with spontaneous formation of current sheets in an AR cluster makes it very productive in flare/CME occurrence. Moreover, the evidence of flare/CME initiation led by the eruption of inter-connecting loops or channeling filaments of the connected ARs had not been clearly described before.

It is well-known that the large-scale pattern of solar AR distribution on the Sun has been studied since the late 1940s (see Bumba and Howard [31]). Activity complex (complex of activity) was defined as a cluster or sequence of ARs which were related by the proximity and continuity of flux emergence (Gaizauskas et al. [32]), and they formed in a month with lifetime of 3–6 solar rotations. In some sense, the AR cluster might serve as an ingredient of an activity complex. However, the latter was defined as the AR distribution pattern with a statistical basic. In this paper an AR cluster is referred to physically connected two or more ARs which happened to appear on the Sun, more or less, simultaneously. Combining the statistical study on activity complex and the detailed analysis of the AR clusters possibly in an activity complex may lead to better understanding of the physics of solar activity.

1 Wang J X, Zhou G P, Wen Y Y, et al. Transequatorial filament eruption and its link to a coronal mass ejection. Chin J Astron Astrophys, 2006, 6: 247–259

2 Wang J X, Zhang Y Z, Zhou G P, et al. Solar trans-equatorial activity. Solar Phys, 2007, 244: 75–94

3 Zhang Y Z, Wang J X, Attrill G D R, et al. Coronal magnetic connectivity and EUV dimmings. Solar Phys, 2007, 241: 329–349

4 Zhou G P, Wang J X, Wang Y M, et al. Quasi-simultaneous flux emergence in the events of October November 2003. Solar Phys, 2007, 244: 13–24

5 Schrijver C J, Title A M. Long-range magnetic couplings between solar flares and coronal mass ejections observed by SDO and STEREO. J Geophys Res, 2011, 116: A04108

6 Schrijver C J, Title A M, Yeates A R, et al. Pathways of large-scale magnetic couplings between solar coronal events. Astrophys J, 2013, 773: 93

7 Pesnell W D, Thompson B J, Chamberlin P C. The solar dynamics observatory (SDO). Solar Phys, 2012, 275: 3–15

8 Woods T N, Hock R, Eparvier F, et al. New solar extreme-ultraviolet irradiance observations during flares. Astrophys J, 2011, 739: 59

9 Woods T N. Extreme ultraviolet late-phase flares: Before and during the Solar Dynamics Observatory Mission. Solar Phys, 2014, 289: 3391–3401

10 Lemen J R, Title A M, Akin D J, et al. The atmospheric imaging assembly (AIA) on the solar dynamics observatory (SDO). Solar Phys, 2012, 275: 17–40

11 Wang J X, Jiang J. Magnetohydrodynamic process in solar activity.

Theor Appl Mech Lett, 2014, 4: 052001

12 Zhang Y Z, Hu Y Q, Wang J X. Double catastrophe of coronal flux rope in quadrupolar magnetic field. Astrophys J, 2005, 626: 1096–1101

13 Zhang Y Z, Wang J X, Hu Y Q. Two-current-sheet reconnection model of interdependent flare and coronal mass ejection. Astrophys J, 2006, 641: 572–576

14 Zhang Y Z, Wang J X. A catastrophic flux rope in a quadrupole magnetic field for coronal mass ejections. Astrophys J, 2007, 663: 592–597

15 Longcope D W, Forbes T G. Breakout and tether-cutting eruption models are both catastrophic (sometimes). Solar Phys, 2014, 289: 2091–2122

16 Kliem B, Lin J, Forbes T G, et al. Catastrophe versus instability for the eruption of a toroidal solar magnetic flux rope. Astrophys J, 2014, 789: 46

17 Yan Y H, Sakurai T. New boundary integral equation representation for finite energy force-free magnetic fields in open space above the Sun. Solar Phys, 2000, 195: 89–109

18 He H, Wang H N, Yan Y H. Nonlinear force-free field extrapolation of the coronal magnetic field using the data obtained by the Hinode satellite. J Geophys Res, 2011, 116: A01101

19 Zhang J, Wang J X, Deng Y Y, et al. Magnetic flux cancellation associated with the major solar event on 2000 July 14. Astrophys J, 2001, 548: L99–L102

20 Wang J X, Zhou G P, Zhang J. Helicity patterns of coronal mass ejection-associated active regions. Astrophys J, 2004, 615: 1021–1028

21 Wang J X, Zhao M, Zhou G. Magnetic changes in the course of the X7.1 solar flare on 2005 January 20. Astrophys J, 2009, 690: 862–874

22 Wen Y Y, Wang J X, Maia D J F, et al. Spatial and temporal scales of coronal magnetic restructuring in the development of coronal mass ejections. Solar Phys, 2006, 239: 257–276

23 Zhang Y, Zhang M, Zhang H Q. A statistical study on the relationship between surface field variation and CME initiation. Adv Space Res, 2007, 39: 1762–1766

24 Chen A Q, Wang J X, Li J W, et al. Statistical properties of superactive regions during solar cycles 19–23. Astron Astrophys, 2011, 534: A47

25 Chen A Q, Wang J X. Quantifying solar superactive regions with vector magnetic field observations. Astron Astrophys, 2012, 543: A49

26 Nitta N V, Liu Y, DeRosa M L, et al. What are special about ground-level events? flares, CMEs, active regions and magnetic field connection. Space Sci Rev, 2012, 171: 61–83

27 Vemareddy P, Ambastha A, Maurya R A, et al. On the injection of helicity by the shearing motion of fluxes in relation to flares and coronal mass ejections. Astrophys J, 2012, 761: 86–103

28 Grechnev V V, Uralov A M, Slemzin V A, et al. A challenging solar eruptive event of 18 November 2003 and the causes of the 20 November geomagnetic superstorm. I. unusual history of an eruptive filament. Solar Phys, 2014, 289: 289–318

29 Wang J X, Ji H S. Recent advances in solar storm studies in China. Sci China-Earth Sci, 2013, 56: 1091–1117

30 Low B C. Field topologies in ideal and near-ideal magnetohydrodynamics and vortex dynamics. Sci China-Phys Mech Astron, 2015, 58: 015201

31 Bumba V, Howard R. Large-scale distribution of solar magnetic fields. Astrophys J, 1965, 141: 1502–1512

32 Gaizauskas V, Harvey K L, Harvey J W, et al. Large-scale patterns formed by solar active regions during the ascending phase of cycle 21. Astrophys J, 1983, 265: 1056–1065